Influence of Retained Austenite on Short Fatigue Crack Growth and Wear Resistance of Case Carburized Steel

V.F. da Silva, L.F. Canale, D. Spinelli, W.W. Bose-Filho, and O.R. Crnkovic

(Submitted 21 August 1998; in revised form 6 July 1999)

The influence of the amount of retained austenite on short fatigue crack growth and wear resistance in carburized SAE 8620 steel was studied in this article. Different amounts of retained austenite in the microstructure of the carburized case were obtained through different heat treatment routes applied after the carburizing process. The wear tests were carried out using pin on disk equipment. After every 200 turns the weight loss was registered. Four point bend fatigue tests were carried out at room temperature, using three different levels of stress and $R = 0.1$. Crack length versus number of cycles and crack growth rate versus mean crack length curves were analyzed. In both tests the results showed that the test pieces with higher levels of retained austenite in the carburized case exhibited longer fatigue life and better wear resistance.

Keywords carburized case, fatigue, retained austenite, SAE 8620 steel, wear

1. Introduction

Case carburized steels can present a microstructural composition, which results in high superficial hardness and an increased mechanical, fatigue, and wear strength. The combination of these properties is recommended for applications where high stress and cyclic loading are involved, such as shafts, housing, and gears (Ref 1). Case carburized steels present a very complex microstructure. Close to the surface, it is composed of high carbon tempered martensite, retained austenite, and carbides. The retained austenite is a very ductile phase, and its presence in the microstructure has been a controversial subject in controlling both wear and fatigue behavior. High amounts of retained austenite in the carburized case may decrease the wear resistance or the contact fatigue in the gears (Ref 2). However, some researchers (Ref 3, 4), suggested that due to the strain induced austenite-martensite transformation, the presence of retained austenite may have some beneficial effect on the flexural fatigue, while Hu et al. (Ref 5) suggest that the austenite will transform into brittle martensite, accelerating the crack propagation and decreasing fatigue resistance. The amount of the retained austenite in the carburized case may vary as a function of the carburizing process and heat treatment applied, and its effect on the mechanical properties is directly related to its amount and distribution on the microstructure, as well as the type of loading to which the carburized material will be submitted. The main goal of this study was to evaluate the influence of different levels of retained austenite on the performance of case carburized SAE 8620 steel during abrasive wear and flexural fatigue.

V.F. da Silva, L.F. Canale, D. Spinelli, W.W. Bose-Filho, and **O.R. Crnkovic,** Materials, Aeronautic, and Automotive Engineering Department, Engineering School of Sao Carlos, Sao Carlos—SP, Brazil. Contact e-mail: waldek@sc.usp.br.

2. Experimental Procedure

2.1 Materials

All specimens were removed from a SAE 8620 structural steel and hot milled to a 19 mm round bar. Table 1 presents the chemical composition.

The specimens were preheated in a furnace at 400 °C for 40 min and transferred to a salt bath furnace at 930 °C for carburizing for 3 h. After the carburizing process, the specimens were divided into two groups for wear (routes A, B, and C) and fatigue (routes D, E, F, and G) tests, and they were submitted to the following heat treatments:

- *Route A:* Austenitization at 840 °C for 20 min, followed by a martempering treatment in a salt bath furnace at 160 °C for 20 min, tempered at 160 °C for 2 h, and cooled in air to room temperature
- *Route B:* Austenitization at 840 °C for 20 min, followed by a martempering treatment in a salt bath furnace at 160 °C for 20 min, tempered at 160 °C for 2 h, cooled in liquid nitrogen at –196 °C, and tempered again at 160 °C for 1 h
- *Route C:* Austenitization at 800 °C for 20 min, followed by a martempering treatment in a salt bath furnace at 160 °C for 20 min, tempered at 160 °C for 2 h, and cooled in air to room temperature
- *Route D:* Same as route A

Table 1 Chemical composition of SAE 8620

Element	Composition, wt%
C	0.22
Mn	0.84
Si	0.26
Ni	0.48
Cr	0.53
Mo	0.16
P	0.018
S	0.021

- *Route E:* Austenitization at 840 °C for 20 min, followed by a martempering treatment in a salt bath furnace at 160 °C for 20 min, tempered at 240 °C for 2 h, and cooled in air to room temperature
- *Route F:* Martempering treatment directly from 930 °C in a salt bath furnace at 160 °C for 20 min; first tempering treatment at 160 °C for 2 h, preheated at 400 °C, and austenitized at 840 °C for 20 min; second tempering treatment at 160 °C for 2 h and cooled in air to room temperature
- *Route G:* Austenitization at 840 °C for 20 min, followed by a martempering treatment in a salt bath furnace at 160 °C for 20 min, tempered at 160 °C for 2 h, cooled in liquid nitrogen at –196 °C, and tempered again at 160 °C for 2 h

After the heat treatments, samples were removed from each group for microstructural, hardness measurement, and x-ray analysis to evaluate the amount of retained austenite.

2.2 Abrasive Wear Test

The specimens for the abrasive wear test were machined to a 12 mm diameter and 15 mm high cylinder, with both faces ground to warranty the necessary alignment. Six specimens from each heat treatment (A, B, and C) were tested using a pin on disk machine with a rotational speed of 53 rpm, contact pressure of 0.03 MPa, and 220 mesh silicon carbide paper. All specimens were tested for 1400 turns, and at each 200 turns, the test was interrupted for mass measurement.

2.3 Fatigue Test

Four point bend fatigue tests were used to analyze the behavior of short cracks. As can be seen from Fig. 1, in this type of loading, the maximum stress is concentrated on the testpiece surface, and it is constant in the space between the two inner loading points. For the fatigue test, 40 specimens were machined to 8 by 10 mm^2 cross section and 100 mm length. The specimens edges were slightly rounded to reduce any heterogeneity related to carbon content in the carburized case. The fatigue tests were completed at room temperature, using load control; sinoidal wave; stress ratio, $R = 0.1$; and 3 Hz frequency.

For the stress evaluation on the surface, the following equation was used:

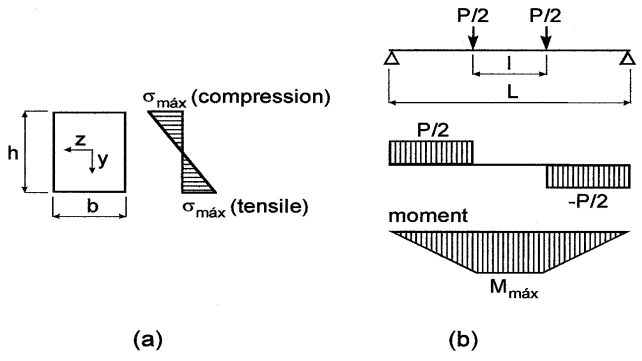

Fig. 1 (a) Stress distribution. (b) Shear load distribution and the equivalent moment

$$\sigma = \frac{3}{2}(L - l)\frac{P}{bh^2} \quad \text{(Eq 1)}$$

where σ is the stress on the surface under tension; L is the distance between the external rollers, 80.0 mm; l is the distance between the inner rollers, 10.0 mm; P is the applied load; b is the testpiece width, 10.0 mm; and h is the testpiece height, 8.0 mm.

The specimens were loaded in four point bending with different stress amplitude, σ_a = 1107, 1181, and 1255, which gave three maximum stresses at the surface, σ_{max} = 1230, 1312, and 1394. During the test, periodically the specimens were loaded at the mean fatigue load to allow measurement of the short fatigue cracks initiation and propagation by acetate replication technique. The fatigue tests ended only after complete failure of the specimen. From these tests the maximum stress versus number of cycles, *S-N* curves; crack size, 2*c*, versus number of cycles; and the crack growth rate, $d2c/dN$, versus the mean size of the crack, $2c_{mean}$, curves were obtained. The crack growth rates were evaluated using the secant method, as previously shown by Boabaid (Ref 6) and De Los Rios et al. (Ref 7), that is:

$$\frac{d2c}{dN} = \frac{2c_{n+1} - 2c_n}{N_{n+1} - N_n} \quad \text{(Eq 2)}$$

Boabaid (Ref 6), showed that the evaluation of the crack growth rate is more representative when it is made between two stages. Therefore, for the crack mean size evaluation, the following equation was used:

$$2c_{medio} = \frac{1}{2}(2c_{n+1} + 2c_n) \quad \text{(Eq 3)}$$

3. Results and Discussion

3.1 Microstructure

The microstructural evaluation from the carburized case (Fig. 2) showed that after the carburizing process, the heat treatments applied promoted microstructures composed of high carbon tempered martensite, retained austenite, and carbides. These microstructures presented a large variation in the amount of retained austenite and in the prior austenite grain size, depending of the applied heat treatment. From the x-ray diffraction pattern results, Table 2, it was possible to see that the samples treated by routes A, D, and F contained a relatively high amount of retained austenite, approximately 36, 35, and 32%, respectively. Those treated by routes C and E contained about 23 and 15%, respectively, and those treated by routes B and G contained less than 6% retained austenite. The differences between the amount of retained austenite obtained from routes C and E and those obtained from routes A, D, and F were mainly due to austenitization temperature (800 °C for route C) and tempering temperature (240 °C for route E).

The tempering temperature for routes A, D, and F is inside the first range of tempering temperatures (150 to 200 °C), where only stress release and carbide formation is promoted. It

has been reported (Ref 1), that carburized steel tempered in this range of temperatures exhibit excellent mechanical properties. Route E produced a lesser amount of retained austenite due to a higher tempering temperature, 240 °C, which is located inside the second range of tempering temperature, where the total or partial transformation of the retained austenite into ferrite and carbides may occur. The subzero heat treatment in routes B and G promoted the lowest amount of retained austenite, which was transformed into martensite. In these routes the first tempering was executed to reduce the risk of cracking in the carburized case.

By comparing all the microstructures obtained from routes D, E, F, and G (Fig. 2), route F promoted the most refined microstructure, and consequently, the retained austenite appeared finely distributed on the matrix. This grain refinement, occurring during the second austenitization at 840 °C, was mainly due to the martensitic microstructure formed during the first martempering treatment. It was also observed that the shape of the carbides presented a strong tendency to change from elongated to a spherical shape.

The different heat treatment routes resulted in a small variation in the hardness values (Table 2). For carburized case microstructures obtained from routes D, F, and G, with a tempering temperature of 160 °C, a normal trend was found, that is, as the amount of retained austenite increased the hardness value decreased. Route E presented a microstructure with the lowest hardness value due to the high tempering temperature of 240 °C that caused a major effect on the martensite. This softening effect was superior to the hardening effect caused by the retained austenite to martensite phase transformation.

3.2 Abrasive Wear

From Fig. 3, it is possible to observe that until the test time of 15 min all test pieces presented an increase in the wear rate, and test pieces from routes A and C (with 37 and 23% of retained austenite, respectively) presented the same wear behav-

Table 2 Amount of retained austenite, %

Heat treatment	Hardness, HRC	Retained austenite, %
A	59.7 ± 1.8	37
B	62.7 ± 1.2	Less than 6
C	61.4 ± 1.5	23
D	61.0 ± 2.0	35
E	59.6 ± 1.0	15
F	61.0 ± 1.0	32
G	63.7 ± 1.2	Less than 6

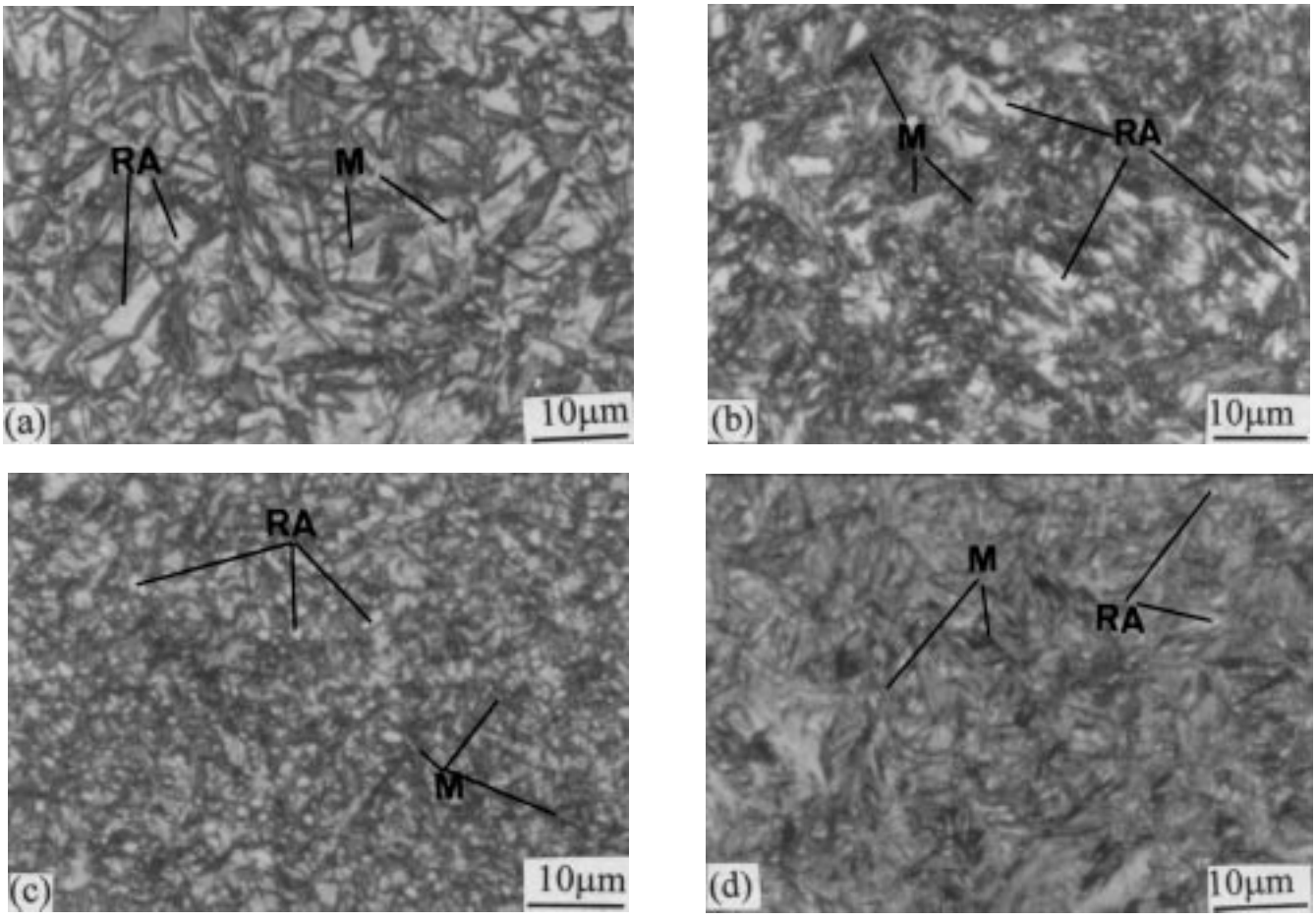

Fig. 2 Optical microscopy, showing the microstructure in the carburized case, from test pieces after carburizing and heat treatments following routes: (a) D, (b) E, (c) F, and (d) G. RA, retained austenite; M, martensite

ior with better wear performance than the test piece from route B (less than 6% of retained austenite). After this time, there was a change in the wear regime, that is, from running in to equilibrium wear regime. This is mainly due to the system tribological characteristics, where the abrasive wear capacity is reduced with time. Also, the test piece from the start of route A presented a lower tendency in loss of mass. Therefore, for the test parameters used, these results showed that the presence of retained austenite in the carburized case increased the abrasive wear resistance.

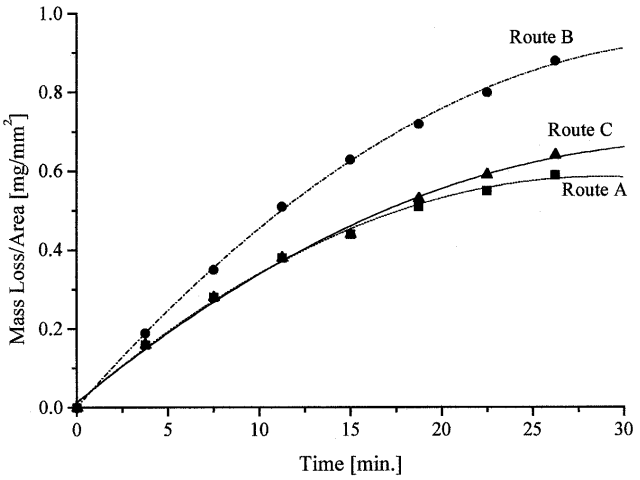

Fig. 3 Mass loss/area versus testing time

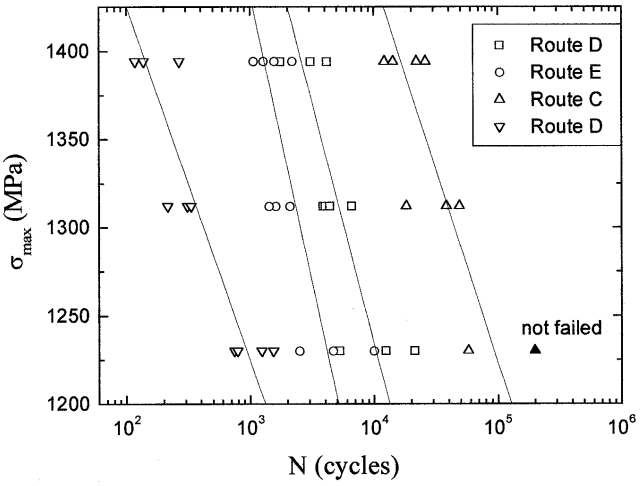

Fig. 4 Four point bend fatigue tests, $R = 1$. Stress versus number of cycles of curves for routes D, E, F, and G

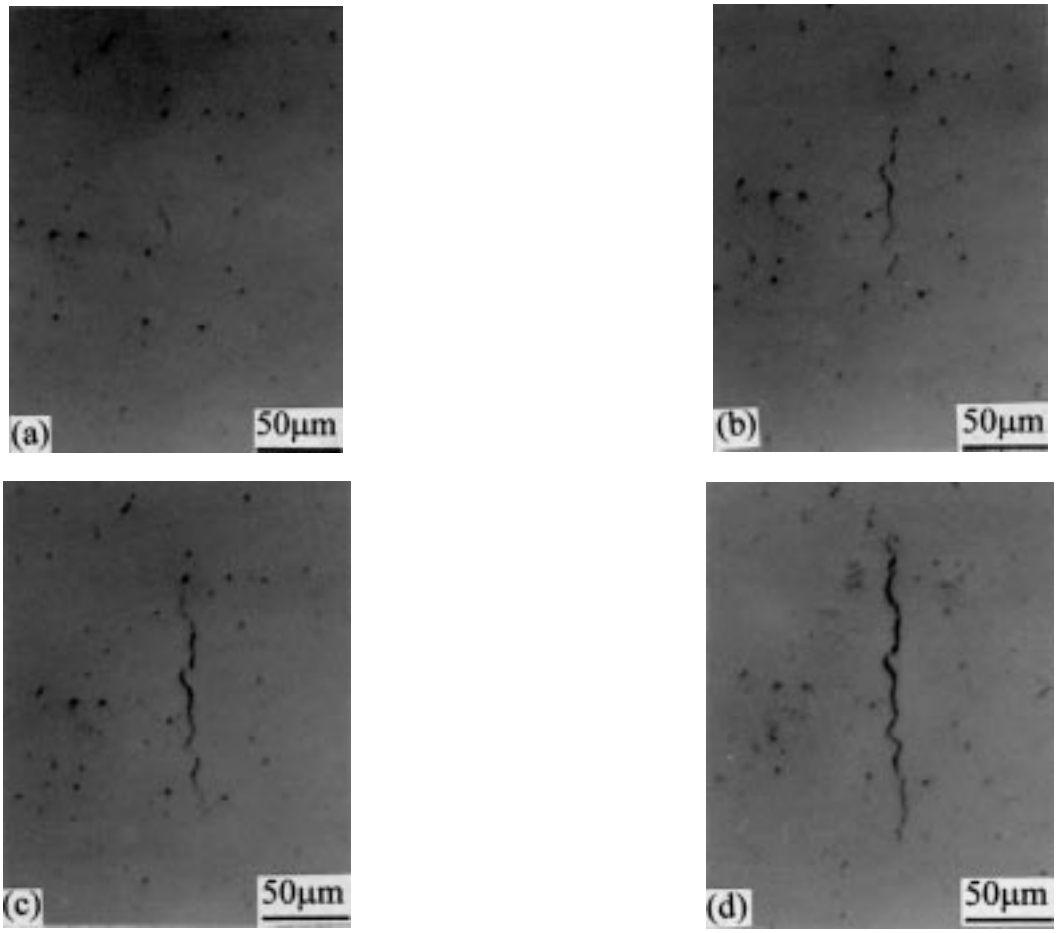

Fig. 5 Fatigue crack nucleation and growth recorded by acetate replication technique. $\Delta\sigma = 1181$ MPa. Total cycles number/crack size ($2c$). (a) 300/30 μm. (b) 900/90 μm. (c) 1100 μm. (d) 1500/190 μm

3.3 *Fatigue*

The *S-N* curves obtained from the fatigue tests (Fig. 4) show that the routes that produced a relatively large amount of retained austenite in the microstructure of the carburized case also resulted in a longer fatigue life.

Using a repetitive replication technique, as shown in Fig. 5, it was possible to observe and measure the microcrack size and correlate it to the number of cycles. The same behavior observed in the *S-N* curves was also found in this case (Fig. 6). Routes D and F had higher fatigue life than routes E and G. This means that the retained austenite may promote a lower crack growth rate, and it may be responsible for an early fatigue threshold. The superior performance exhibited by the microstructure obtained by route F, when compared to route D, is due to a more refined microstructure obtained from route F. Hyde et al. (Ref 8) found that the size of the austenitic grain in the car-

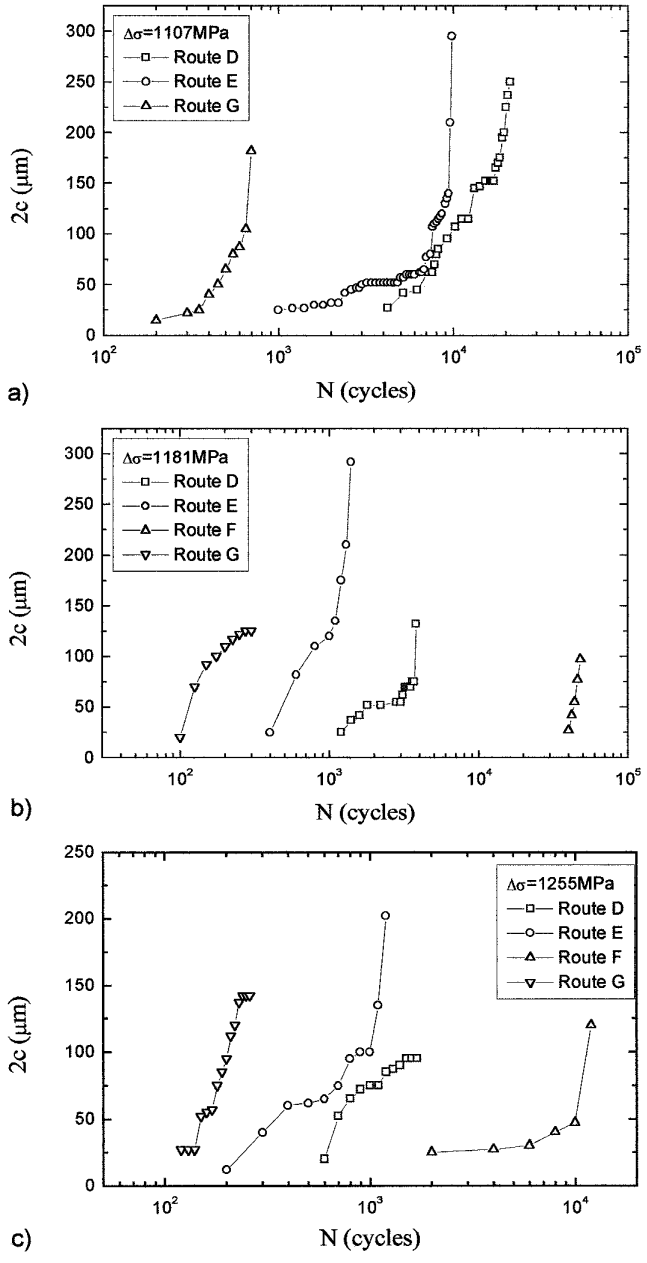

Fig. 6 Crack size versus number of cycles. (a) Δσ = 1107 MPa. (b) Δσ = 1181 MPa. (c) Δσ = 1255 MPa

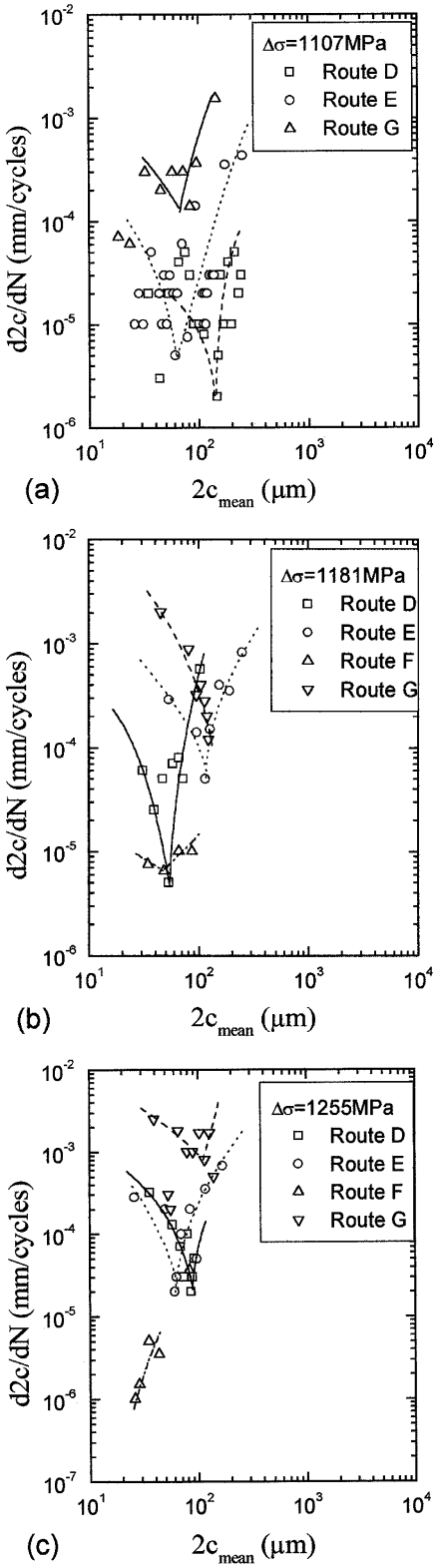

Fig. 7 Crack growth rate versus crack mean size. (a) Δσ = 1107 MPa. (b) Δσ = 1181 MPa. (c) Δσ = 1255 MPa

burized case influences the fatigue life in a way similar to that of the grain size in the Hall-Pech equation, and the fatigue life is directly proportional to the inverse of the square root of the grain, ($d^{-1/2}$). Another important factor is that during crack propagation, the microstructure can act as a barrier, and the most refined microstructure presents the smaller space between each barrier (grain boundaries, spherical particles, and martensite colonies), which makes the crack spend more energy to grow (Ref 7).

Considering the crack growth versus the crack mean size curves (Fig. 7), the influence of the retained austenite on the crack growth rate is not completely clear. However, when compared with microstructure obtained from route G, it was possible to observe a tendency in microstructures from routes F and D to present a lower $2c_{th}$ and a lower crack growth rate $d2c/dN$.

For the test conditions used in this work, flexural low cycle fatigue and the presence of retained austenite in the carburized case microstructure, a beneficial effect in increasing fatigue life is shown. Generally, the improvement in the fatigue life is attributed to both the capacity of the retained austenite to transform in martensite during the local plastic deformation process and the presence of compressive residual stress originated during this phase transformation. When retained austenite transforms to martensite, there is an increase in volume, which causes the appearance of compressive stresses, and their level is dependent of the retained austenite carbon content before the phase transformation. Some researchers (Ref 4, 9, 10) observed this type of phase transformation in carburized case steel after low cycle fatigue tests. Gu et al. (Ref 11) and Lou et al. (Ref 12) performed fatigue crack growth tests in carburized steels and observed a reduction in the crack growth rate in test pieces with high retained austenite content in the carburized case. They attributed this fact to both the induced plastic strain austenite-martensite phase transformation and the crack closure caused by the compressive residual stress generated during this transformation that occurred in the plastic zone ahead of the crack tip.

From the fracture surface analysis, it was noticed that the crack growth mode was transgranular through the carburized case in all specimens. This micromechanism of fatigue crack growth is related to microstructures of fine grains and high fatigue limit (Ref 1).

The specimens with higher retained austenite in the carburized case (routes D and F), exhibited relatively high hardness values, better wear performance, and larger fatigue life, particularly the specimens from route F. However, for the routes that resulted in a low amount of retained austenite, due to higher tempering temperature or subzero treatment, a reduction in the wear performance and fatigue life was found. The improvement in the wear performance may be related to both the hardening effect of the retained austenite and/or the strain induced ability of retained austenite to transform into martensite during abrasion. In the fatigue results, this was attributed to the strain induced phase transformation micromechanism of the retained austenite into martensite, which may have promoted crack closure at the crack tip, reducing the crack growth rate.

5. Conclusions

In this study the influence of the retained austenite on the wear and fatigue resistance of a case carburized steel were evaluated. The results showed that the presence of retained austenite in the carburized case increased the abrasive wear resistance and improved the fatigue life in low cycle fatigue tests.

Acknowledgment

The financial support from CNPq and FAPESP—Brazil is gratefully acknowledged.

References

1. G. Krauss, Microstructure, Residual Stress, and Fatigue of Carburized Steels, *Proceedings: Quenching, and Carburizing* (Melbourne), The Institute of Materials, 1991, p 205-225
2. J.V. Faria, Silva, 1993, Master Report—Escola Politécnica, Universidade de São Paulo, Brazil
3. G. Krauss, Microstructure and Performance of Carburized Steel. Part III: Austenite and Fatigue, *Adv. Mater. Process.*, Vol 148 (No. 3), 1995, p 42EE-42II
4. M.A. Zaccone, J.B. Kelley, and G. Krauss, Fatigue and Strain Hardening of High Carbon Martensite-Austenite Composite Microstructures, *Proceedings Heat Treatment '87*, The Institute of Metals, 1987, p 93-101
5. Z.Z. Hu, M.L. Ma, and J.H. Liu, *J. Fatigue*, Vol 19 (No. 8/9), 1997, p 641-646
6. J.S. Boabaid, "The Effect of Manufacturing Variables on Short Fatigue Crack Growth in Waspaloy at 19 °C," Second Progress Report, University of Sheffield, Sheffield, 1993
7. E.R. De Los Rios, A. Walley, M.T. Milan, and G. Hammersley, Fatigue Crack Initiation and Propagation on Shot Peened Surfaces in A316 Stainless Steel, *Int. J. Fatigue*, Vol 17 (No. 7), 1995, p 493-499
8. R.S. Hyde, G. Krauss, and D.K. Matlock, Phosphorus and Carbon Segregation: Effects on Fatigue and Fracture of Gas Carburized Modified 4320 Steel, *Metal. Mater. Trans. A*, Vol 25 (No. 6), 1994, p 1229-1240
9. Z. Mei and J.W. Morris, Influence of Deformation-Induced Martensite on Fatigue Crack-Propagation in 304 Type Steels, *Metal. Trans. A*, Vol 21 (No. 12), 1980, p 3137-3152
10. M.A. Panhans and R.A. Fournelle, High Cycle Fatigue Resistance of AISI E9310 Carburized Steel with Two Different Levels of Surface Retained Austenite and Surface Residual Stress, *J. Heat Treat.*, Vol 2 (No. 1), 1981, p 54-61
11. C. Gu, B. Lou, X. Jing, and F. Shen, Mechanical Properties of Carburized Cr-Ni-Mo Steels with Added Case Nitrogen, *J. Heat Treat.*, Vol 7 (No. 2), 1989, p 87-94
12. B. Lou, X. Jing, C. Gu, F. Shen, and L. He, Fatigue Crack Growth and Closure Behaviors in Carburized and Hardened Case, *Proceedings Fatigue '90* (Honolulu), Birmingham, Materials and Component Engineering Publications, 1990, p 1161-1166